

## Speciation of osmium in an iron meteorite and a platinum ore specimen based on X-ray absorption fine-structure spectroscopy

NAOKI SAKAKIBARA,<sup>1,2</sup> YOSHIO TAKAHASHI,<sup>1,3\*</sup> KAZU OKUMURA,<sup>4</sup> KEIKO H. HATTORI,<sup>5</sup> TSUYOSHI YAITA,<sup>6</sup> KATSUHIKO SUZUKI<sup>7</sup> and HIROSHI SHIMIZU<sup>1,3</sup>

<sup>1</sup>Department of Earth & Planetary Systems Science, Hiroshima University, Higashi-Hiroshima 739-8526, Japan

<sup>2</sup>Japan Food Research Laboratories, Toyotsu, Suita, Osaka 564-0051, Japan

<sup>3</sup>Laboratory for Multiple Isotope Research for Astro-and Geochemical Evolution (MIRAGE), Hiroshima University, Higashi-Hiroshima 739-8526, Japan

<sup>4</sup>Department of Materials Science, Tottori University, Tottori 680-8552, Japan

<sup>5</sup>Department of Earth Sciences, University of Ottawa, Ottawa, ON, K1N 6N5, Canada

<sup>6</sup>Japan Atomic Energy Research Institute, Tokai 319-1195, Japan

<sup>7</sup>Institute for Frontier Research on Earth Evolution (IFREE), Japan Marine Science and Technology Center (JAMSTEC), Yokosuka 237-0061, Japan

(Received August 24, 2004; Accepted April 7, 2005)

We report here the first synchrotron radiation (SR)-based X-ray absorption fine structure (XAFS) spectra for Os at L<sub>III</sub>-edge in geo- and cosmo-chemical materials. Samples were Negrillos meteorite, a II-A type iron meteorite, and a Pt ore specimen, aggregates of coarse grained Pt-Fe alloys, from the Chocó district, Colombia. X-ray absorption near-edge structure (XANES) spectra of Os are presented for Negrillos, which has an Os abundance of 65 ppm, as well as for the platinum-group mineral (PGM). The XANES spectra showed that Os in the iron meteorite and the PGM chiefly exist as a metallic species.

The average interatomic distance of Os in the Pt ore from the Chocó district are calculated from the EXAFS spectra. The results suggest that the neighboring atoms of Os are not Pt. Instead, they are most likely Os and Ir. This is consistent with the common occurrence of fine lamellae of Os and iridosmine as exsolution products of Pt-Fe alloys. Furthermore, this confirms the limited solubility of Os in Pt-Fe alloys. EXAFS could thus be useful for identifying the host phases of Os in natural samples. This study has verified that the chemical state of Os in natural samples can be determined using XAFS. It is expected that further application of the XAFS technique to Os speciation in natural samples will help to elucidate Re/Os fractionation processes in the Re-Os isotopic system.

Keywords: osmium, speciation, iron meteorite, platinum-group mineral (PGM), extended X-ray absorption fine structure (EXAFS), X-ray absorption near edge structure (XANES)

### INTRODUCTION

The chemical-state of elements is important for understanding geo- and cosmochemical processes and for clarifying the origin of geo- and cosmochemical samples and their formation environments. There have been many studies of the speciation of major elements, such as Fe, using Mössbauer spectroscopy (Hawthorne, 1988), but it has been difficult to study the chemical state of trace elements (<1%) in natural rocks. Recent advances in X-ray absorption fine structure (XAFS) using synchrotron radiation (SR) have allowed us to conduct the speciation of trace elements such as Zr, Ce, and Eu in natural rocks

(Farges *et al.*, 1994; Takahashi *et al.*, 2000; Rakovan *et al.*, 2001; Brown and Sturchio, 2002).

Platinum group elements (PGEs), which are highly siderophilic, have been widely studied to understand geochemical processes related to core formation and mantle evolution in the Earth (Fleet *et al.*, 1999; Alard *et al.*, 2000). In particular, Os is of great interest in cosmochemistry and geochemistry, as the Re-Os isotope system provides a unique geo- and cosmochronometer and an isotope tracer. Osmium isotopic ratios are highly variable among rocks due to large Re-Os fractionation during partial melting and fractional crystallization. Recent improvements in analytical techniques for the determination of Re and Os abundances and Os isotopic ratios have promoted Re-Os geochemical studies (Shirey and Walker, 1998). In addition, Os displays variable oxidation states between -2 to +8 and the valence of Os un-

\*Corresponding author (e-mail: ytakaha@hiroshima-u.ac.jp)

doubtedly affects its behavior. There have been no detailed studies using XAFS on the chemical states of Os in natural rocks, such as oxidation state and local atomic structure around Os atoms. Speciation of Os in natural rocks is essential for evaluating the distribution and geochemical behavior of Os at the Earth's surface and interior.

In this study, XAFS spectroscopy was applied to the speciation of Os in two natural samples. A XAFS spectrum consists of two regions, X-ray absorption near edge structure (XANES) and extended X-ray absorption fine structure (EXAFS), which provide different information. XANES may provide the oxidation state and symmetry of a given element, and EXAFS spectra provide information on the local coordination environment of an element. As natural samples, one PGE alloy and one IIA-type iron meteorite were chosen. We report here the successful application of XANES to the speciation of trace Os incorporated in a platinum-group mineral (PGM) and an iron-meteorite (Os: 65 ppm) to determine the oxidation state of Os. In addition, EXAFS was successfully used to determine the local structure around Os in the PGM.

## SAMPLES AND ANALYTICAL METHODS

### Samples

Negrillos, a II-A type iron meteorite, and one Pt ore from the Chocó district, Colombia, were employed. Sample compositions determined by EPMA (JEOL 733) for the Negrillos are given in Table 1, together with the Os, Ir, and Pt abundance data for Negrillos reported by Horan *et al.* (1992) and Wilson *et al.* (1997). Morgan (1971) showed that hexahedrite Negrillos has the highest Os abundance among reported meteorites, referring to the average Os concentration of 50 ppm for meteorite from Herr *et al.* (1961). Horan *et al.* (1992) and Smoliar *et al.* (1996) reported Os concentrations of 65 ppm for Negrillos, confirming that it has the highest Os content among iron meteorites analyzed to date (from 30 iron meteorites by Smoliar *et al.*, 1996, and 12 iron meteorites by Horan *et al.*, 1992). Moreover, the group IIA iron meteorites, to which Negrillos is belongs, are magmatic products and exhibit the widest range in Re/Os ratios among all the iron meteorites (Smoliar *et al.*, 1996; Shirey and Walker, 1998). The Negrillos sample was sliced to about 200  $\mu\text{m}$  in thickness to reduce the scattering X-rays from the Fe-Ni alloy.

A chip of a Pt ore specimen ( $\sim 5$  mm) from the Chocó district was used for the XAFS measurement. The Chocó district is well known for the production of Pt from placers, having been the primary source of Pt for over 200 years before the advent of hard rock mining in South Africa and Canada in 20th century (e.g., Hattori and Cabri, 1991). The Pt ore in the Chocó district consists of coarse-

Table 1. Major element compositions (wt.%) and PGE abundances (ppm) in Negrillos iron meteorite

Fe	90.3
Ni	4.74
Co	0.37
Os	65.3 ppm*
Ir	56.1 ppm**
Pt	122 ppm**
Total	95.4

\*Horan *et al.* (1992).

\*\*Wilson *et al.* (1997).

grained Pt-Fe alloys recovered from tributaries near zoned-type ultramafic-mafic intrusions, so-called Alaskan-type intrusions (e.g., Weiser, 2002).

Four Os reference materials, Os metal, Os(II)S<sub>2</sub>, OsCl<sub>3</sub>, and OsO<sub>4</sub>, were also employed to observe the chemical shift of the absorption edge caused by differences in the Os oxidation state and symmetry. For commercially available compounds such as Os metal, OsCl<sub>3</sub>, and OsO<sub>4</sub>, each reference sample was diluted to 1 wt.% by addition of SiO<sub>2</sub> powder and pressed into a pellet under Ar atmosphere for XAFS analysis. The OsO<sub>4</sub> was doubly sealed in a polyethylene bag to prevent OsO<sub>4</sub> vapor from escaping due to its high volatility. The sample of OsS<sub>2</sub> (erlichmanite) was collected from the residual laterite covering the Freetown Igneous Complex in Sierra Leone. The occurrence and the composition of the sample are described in Hattori *et al.* (1991).

### Analytical methods

XANES and EXAFS spectra for all the samples were measured at beamline BL01B1 of SPring-8 (Hyogo, Japan). The incident X-ray beam was monochromatized by a Si(111) double crystal monochromator, and the beam size at the sample position was less than 1 mm  $\times$  1 mm. Osmium L<sub>III</sub>-edge (10.858 keV) XANES and EXAFS spectra were recorded at room temperature in a transmission mode using ion chambers or in a fluorescence mode using a 19 element Ge semiconductor detector (SSD). In the latter case, the detection system consists of amplifiers (ORTEC572), single channel analyzers (SCA, ORTEC500), and scalars (ORTEC974). SCA windows were tuned to selectively detect Os L $\alpha$  fluorescence selectively. The total photons entering the detector were kept lower than 100 kcps by adjusting the distance between the SSD and the sample.

The XANES spectrum for the Negrillos meteorite was recorded with a 0.3 eV step (2 sec for 1 point) 11 times,

and averaged. In order to reduce the intensity of X-ray fluorescence from major elements of Fe and Ni in Negrillos, aluminum foil was placed between the sample and the SSD for the Os  $L_{III}$ -edge XANES measurement. The XANES spectra for the other samples were typically recorded with a 0.5 eV step size (2 sec for 1 point) around the  $L_{III}$  edge of Os. The energy range for EXAFS measured was 10.36–11.96 keV.

#### XANES and EXAFS data analysis

The X-ray absorption ( $\bar{\epsilon}$ ) defined as  $\bar{\epsilon} = I_F/I_0$  ( $I_F$ : fluorescence X-ray intensity;  $I_0$ : incident X-ray intensity) was plotted against incident X-ray energy. Dead time corrections were made for the SSD counting. Individual scans were averaged after the correction for dead time.

For the XANES data, the background absorption was subtracted using a linear function estimated from a pre-edge region for the spectra obtained by fluorescence mode, while Victoreen equation was used for the spectra obtained by transmission mode. After removal of the pre-edge, the spectra were normalized to unit absorption at a post-edge region.

EXAFS data were analyzed using REX2000 ver. 2.3 (Rigaku Co.) with parameters generated by FEFF7.0 (Zavinsky *et al.*, 1995; Ankudinov and Rehr, 1997), for which initial structural data provided by ATOMS (Ravel, 2001) were used. After background subtraction and normalization, the smooth  $L_{III}$ -edge absorption of Os free atoms was removed using five cubic splines. The energy unit was transformed from keV to  $\text{\AA}^{-1}$  to produce the EXAFS function  $\chi(k)$ , where  $k$  ( $\text{\AA}^{-1}$ ) is the photoelectron

wave vector given by  $\sqrt{2m(E - E_0 / h^2)}$  ( $E$ : the energy of the incident X-ray;  $E_0$ : the threshold energy). The  $E_0$  value was determined from the maximum value in the first derivative of  $\chi(k)$  in the absorption edge region. The  $k^3$ -weighted  $\chi(k)$  function was Fourier transformed from  $k$  ( $1/\text{\AA}$ ) space into  $R$  ( $\text{\AA}$ ) space to give a radial structural function (RSF) in the  $k$  ( $1/\text{\AA}$ ) range  $2.80 \text{\AA}^{-1} < k < 8.65 \text{\AA}^{-1}$  for the Chocó sample. In this study, the  $k$ -region for the Fourier transformation was determined at the point where  $k^3\chi(k)$  was approximately zero. Back Fourier transformation was performed for the first shell of RSF in the  $R$  range  $1.51 \text{\AA} < R < 2.73 \text{\AA}$  for Chocó sample. The theoretical EXAFS function was fitted to back transformed  $k^3$ -weighted  $\chi(k)$  functions using FEFF7.0. The EXAFS analysis gives the coordination number ( $N$ ), the interatomic distance between absorber ( $A$ ) and scatterer ( $S$ ) atoms ( $R_{A-S}$ ), the Debye-Waller term ( $\sigma^2$ ), and the energy offset ( $E_0$ ). The maximum number of parameters for EXAFS fittings ( $N_{\text{free}}$ ) are defined by  $N_{\text{free}} = (2\Delta k \cdot \Delta r)/\pi$  (Stern, 1993), where  $\Delta k$  and  $\Delta r$  are  $k$  region ( $1/\text{\AA}$ ) of Fourier transformation and  $R$  region ( $\text{\AA}$ ) of back Fourier transformation, respectively. The calculated  $N_{\text{free}}$  for

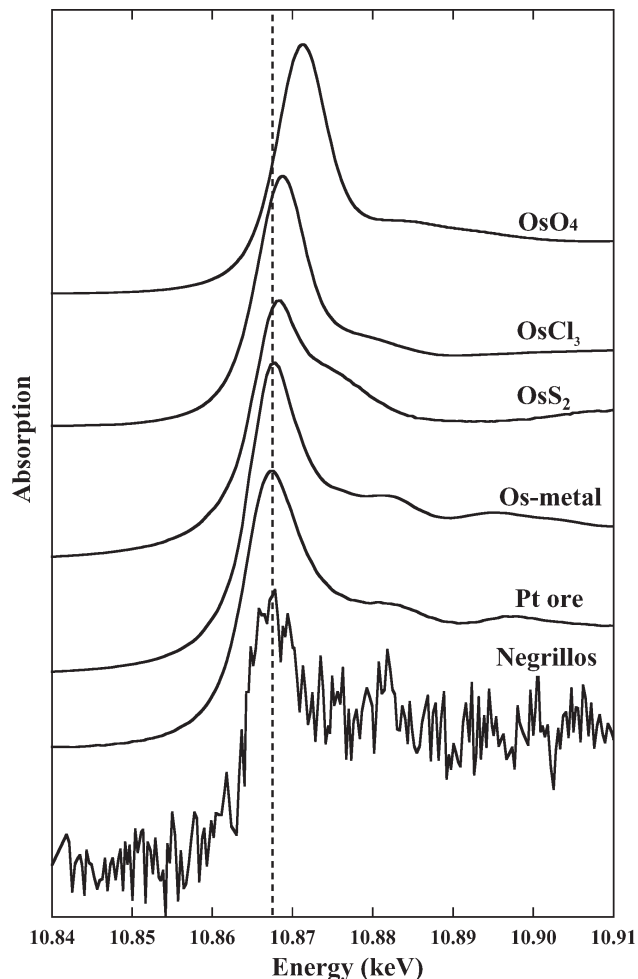


Fig. 1. Osmium  $L_{III}$ -edge XANES spectra of  $\text{OsO}_4$ ,  $\text{OsCl}_3$ ,  $\text{OsS}_2$ ,  $\text{Os-metal}$ , the Pt ore from the Chocó district, and Negrillos iron meteorite. The vertical dotted line marks the position of white line of  $\text{Os-metal}$ .

Chocó sample was 6.

In order to confirm whether our experiments and EXAFS analyses using FEFF are correct, the EXAFS spectra of  $\text{Os-metal}$  and  $\text{OsS}_2$  were also measured as reference materials. The accuracies in the fitted parameters were estimated to be  $\pm 0.02 \text{\AA}$  for  $R$ ,  $\pm 20\%$  for  $N$ ,  $\pm 20\%$  for  $\sigma^2$  (O'Day *et al.*, 1994). The quality of the fit was given by the goodness-of-fit parameter  $R$ , defined by

$$R(\%) = \frac{\sum \{k^n \chi_{\text{obs}}(k) - k^n \chi_{\text{cal}}(k)\}^2}{\sum \{k^n \chi_{\text{obs}}(k)\}^2},$$

where  $\chi(k)_{\text{obs}}$  and  $\chi(k)_{\text{cal}}$  are experimental and theoretical data points, respectively.

## RESULTS AND DISCUSSION

### *XANES analysis of Negrillos iron meteorite and Pt ore in the Chocó District*

Figure 1 shows Os  $L_{III}$ -edge XANES spectra for the Pt ore in PGM in the Chocó District and Negrillos iron meteorite, together with those for the four Os species references. The white line peaks for  $OsO_4$ ,  $OsCl_3$ ,  $Os(II)S_2$ , and Os-metal were observed at 10.871, 10.869, 10.868, and 10.867 keV, respectively (Fig. 1). The shift in the peak position of the XANES spectra, which is common in XANES for many other elements, is explained by the different oxidation state and symmetries around Os in the reference materials. It is suggested that the peak position at higher energy reflects Os at higher oxidation state.

The XANES spectrum for Os in the Chocó specimen showed quite similar features to that for the Os-metal such as peak position of white line at 10.867 keV, a shoulder at 10.886 keV, and a broad peak around 10.890 keV. These results confirm that Os is present as a metallic phase in the alloy. The peak energy of white line of Os in the Os  $L_{III}$ -edge XANES spectrum of Negrillos is identical to that of Os-metal (Fig. 1). In addition, the XANES of Negrillos has a shoulder around 10.886 keV, which is similar to Os-metal and the Os in the Pt ore from the Chocó district. These results support the conclusion that Os is incorporated in a metallic phase in Negrillos.

It is possible that iron meteorites can provide information on the chemical composition and the evolution of Earth's core, as well as mantle-core interaction. Partitioning of Os between the mantle and core could largely depend on the chemical state of Os, particularly Os-metal or Os-sulfide. There have been no data on the chemical speciation of Os in iron meteorites. Our present data suggest that Os in the core may be mainly in metallic form, which may give a constraint on models for evolution of the Earth's core.

### *EXAFS analysis of the Pt ore from the Chocó sample*

The local structure of Os in the Chocó sample was examined using Os  $L_{III}$  edge EXAFS spectroscopy. The quality of EXAFS spectrum of Os in Negrillos was not good enough to yield interatomic distance because of its low Os abundance. Figure 2 shows the  $k^3$ -weighted EXAFS spectra of Os in the Os metal,  $OsS_2$ , and the Pt ore from the Chocó district. The EXAFS function,  $k^3\chi(k)$ , of Os  $L_{III}$ -edge was not obtained up to high  $k$  range ( $\sim 12 \text{ \AA}^{-1}$ ), as the EXAFS spectrum of Ir  $L_{III}$ -edge at 11.21 keV interferes with that of Os  $L_{III}$ -edge in the higher  $k$  region in the sample.

First, the FEFF analyses of Os-metal and  $OsS_2$  reference materials are discussed. Figure 3a shows the  $k^3$ -weighted EXAFS spectra and a fitted curve using FEFF for Os-metal employed as a reference material. The structural parameters given by the EXAFS are shown in

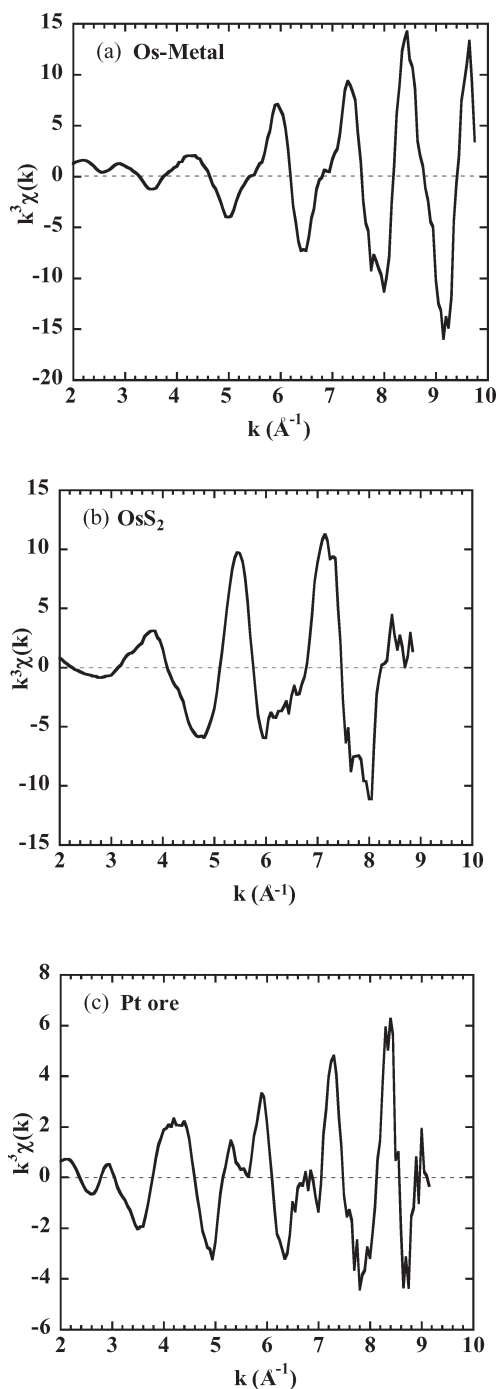


Fig. 2. The  $k^3$ -weighted Os  $L_{III}$ -edge EXAFS spectra for two reference materials (Os metal and  $OsS_2$ ) and the Pt ore sample from the Chocó district.

Table 2. The calculated Os-Os interatomic distance ( $R_{Os-Os}$ : 2.694 Å) and coordination number ( $N = 11.5$ ) determined by the analysis of the Os-metal reference are consistent with the average Os-Os bond length of 2.701 Å for Os metal determined by X-ray diffractometer and

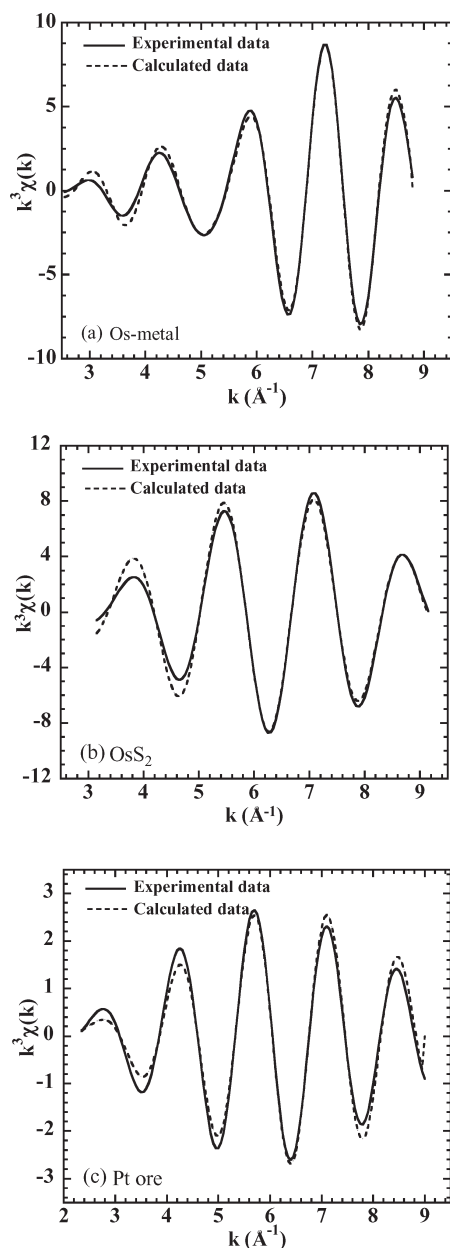


Fig. 3. The  $k^3$ -weighted Os  $L_{III}$ -edge EXAFS spectra (solid line) after back Fourier transformation: (a) Os-metal, (b)  $OsS_2$ , and (c) Pt ore from Chocó district. The dashed curves are the fits to the experimental data using FEFF7.0. The structural model for the Pt ore sample assumed Os as first neighboring atom.

its coordination number ( $N$ ) of 12 (Swanson and Ugrinic, 1955).  $OsS_2$  reference material yielded the distance of 2.337 Å between Os and S (Fig. 3b) and the coordination number of 5.6. The values are again comparable with the reported values of 2.351 Å and  $N = 6$  based on a crystallographic study by X-ray diffraction (Stingl *et al.*, 1992). These results confirm that our experiments and structural analysis by FEFF 7.0 are acceptable.

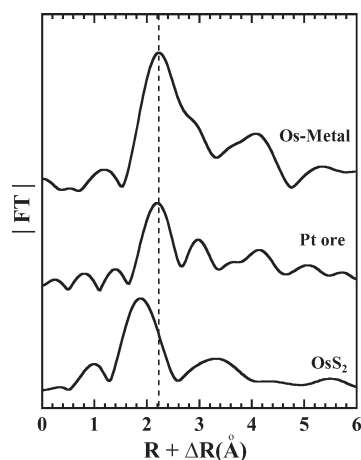


Fig. 4. Radial structure functions for Os metal and the ore minerals. The largest peaks in the figure correspond to the distance between Os and the closest atomic shell. Note that the phase shifts of RSF related to the absorber-scatterer interaction were not corrected.

The radial structural functions (RSF) obtained by the absolute values of Fourier transforms of  $k^3$ -weighted EXAFS are shown in Fig. 4. Comparison of the RSF of the reference Os metal and the Chocó sample indicates that the distance to the first neighboring atom of Os in the Chocó sample is similar to that in Os metal. The  $k^3$ -weighted EXAFS functions obtained by Fourier back-transforming and calculated data using FEFF are shown in Fig. 3c. The XANES analysis showed that Os is in a metallic form in the Pt ore from the Chocó district. Based on this information, Os, Ir, Pt, and Ru are considered as neighboring atoms, which were found in the zoned type PGM samples (Hattori and Cabri, 1991).

The EXAFS spectrum of Chocó sample was initially fitted by Os shell (Fig. 2), the initial parameter of which was obtained by FEFF based on a model where Os ( $N = 12$ ; hexagonal) was considered as first neighboring atom. Optimized parameters show the coordination number of 11.7 and interatomic distance of 2.693 Å (Table 2). The values are comparable with those of Os metal ( $N = 12$ ;  $R_{Os-Os} = 2.701$  Å). The EXAFS spectrum can be also fitted by a model assuming Ir as the first neighboring atom to the absorber Os (Table 2), where Os was treated as a doped atom in the cubic structure of Ir with the coordination number of 12. The optimal Os-Ir distance ( $=2.694$  Å) is reasonably close to the theoretical distance of 2.708 Å based on the metallic bond radii of Ir (1.358 Å; Swanson and Ugrinic, 1955) and Os (1.351 Å). The results suggest that either bonding of Os-Os or Os-Ir is acceptable since EXAFS cannot distinguish atoms having similar atomic numbers. The EXAFS spectra can also be fitted by the parameters assuming Pt ( $N = 12$ ; cubic) in the first shell.

Table 2. EXAFS structural parameters using FEFF7.0 for Os-metal, OsS<sub>2</sub>, Pt ore from the Chocó district. The structural model for the Chocó sample assumed Os, Ir, or Pt as first neighboring atom for the absorber Os atom. *N* = coordination number; *R* ( $\approx$ ) = interatomic distance;  $\Delta E_0$  = threshold *E*<sub>0</sub> shift in eV;  $\sigma$ : Debye-Waller term. Least squares precisions are given in parentheses.

Sample		Shell	<i>N</i>	<i>R</i> ( $\approx$ )	$\Delta E_0$	$\sigma$	Residual (%)
Os-metal		Os-Os	11.5	2.694	9.6	0.065	0.930
			(1.0)	(0.002)	(0.3)	(0.014)	
OsS <sub>2</sub>		Os-S	5.6	2.337	5.6	0.064	1.460
			(0.2)	(0.004)	(0.5)	(0.004)	
Pt ore	(Chocó district)	Os-Os	11.7	2.693	5.1	0.095	0.582
			(0.7)	(0.010)	(1.3)	(0.007)	
Pt ore	(Chocó district)	Os-Ir	12.1	2.694	6.5	0.095	0.788
			(0.7)	(0.010)	(1.2)	(0.007)	
Pt ore	(Chocó district)	Os-Pt	12.5	2.693	7.1	0.097	1.030
			(0.8)	(0.009)	(1.1)	(0.007)	

Errors in the fitted parameters were estimated to be generally  $\pm 0.02 \approx$  for *R*,  $\pm 20\%$  for *N*,  $\pm 20\%$  for  $\sigma^2$  (O'Day et al., 1994).

However, the Os-Pt distance determined (2.693 Å) is slightly shorter than the sum of the metallic bond radii (2.738 Å) of Os (1.351 Å; Swanson and Ugrinic, 1955) and Pt (1.387 Å; Swanson and Tatge, 1953). Finally, hexagonal Ru (*N* = 12) was considered as the atoms in the first shell, but the EXAFS cannot be fitted by the model. These combined results suggest that Os and Ir are the main first neighboring atoms of Os, but Pt and Ru are unlikely.

The possibility that main species of Os is sulfide in the Chocó sample was rejected by EXAFS analysis. If Os exists as a sulfide in the ore, distinct differences would be found in the interatomic distances given by EXAFS. The RSF for OsS<sub>2</sub> shows a peak around 1.8–1.9 Å (Fig. 4b), which locates at shorter *R* than the peak for the PGM. In addition, XANES spectrum of the PGM sample was different from that of OsS<sub>2</sub> (Fig. 1). These results suggest that sulfide is not main Os species in the sample.

If Os is dissolved in Pt-Fe alloys, Pt should be the neighboring element of Os. The proposed interpretation requires Os in the alloy forms separate phase(s). This is supported by common occurrences of native osmium and iridosmine within Pt-Fe alloys (e.g., Hattori and Cabri, 1991; Cabri, 2002). Based on the crystallographic orientation of Os and iridosmine, it has been proposed that there is a miscibility gap between Pt and Os (e.g., Cabri, 2002). Our results confirm that Pt-Fe alloys have limited solubility of Os and that Os exsolved from Pt-Fe alloys forms own phases.

Identification of the host mineral of Os is essential for understanding Os partitioning in the Earth, as Os is normally incorporated into rocks as a minor component.

Our results confirm that EXAFS reflects the closest neighboring atomic species to Os, while XANES can show the oxidation state (and symmetry) of Os. The information on the chemical state of Os can be a clue to understand the Os host phase. Therefore, it is expected that XAFS including XANES and EXAFS can contribute to the identification of host phase of Os in natural rocks.

## CONCLUSIONS AND SUMMARY

This is the first study where the chemical state of Os in natural rocks has been determined using the XAFS technique, which consists of EXAFS and XANES. It has shown that EXAFS is a useful method for identifying the closest neighboring atoms to Os, which will contribute to the identification of the host phase of Os in rocks. Neighboring atoms of Os were concluded to be alloys of Os and Ir in the Pt ore from Chocó Dist by EXAFS analyses. The possibility that main Os species is sulfide in the PGM was rejected by EXAFS and XANES data. XANES is also a powerful technique for studying the speciation of trace elements in natural rocks. The XANES spectra clearly show that Os in the PGM exists in the metallic state. Moreover, it must be noted that XANES was obtained for trace amounts of Os (65 ppm) in Negrillos, showing that Os is incorporated in a metallic form in the iron meteorite. This information may help us to understand the distribution and behavior of Os in the Earth's core and mantle. Further application of similar techniques to other rocks by future studies will give us important geochemical information on Os behavior.

**Acknowledgments**—We thank Drs. T. Uruga and H. Tanida (JASRI) and Mr. M. Fukukawa (Hiroshima Univ.) for their great contribution to the XAFS experiments and Mrs. Y. Shibata and H. Ishisako (Hiroshima University) for EPMA analyses and Dr. M. Handler (IFREE, JAMSTEC) for valuable comments on the manuscript. Smithsonian National Museum of Natural History is thanked for loaning the iron meteorite chip. Constructive comments by two anonymous reviewers greatly improved this paper. This work has been performed with the approval of SPring-8 (Proposal No. 2001B0393-NX-np). This study was supported by a Grant-in-Aid for Scientific Research from JSPS (Japan Society for the Promotion of Science).

## REFERENCES

- Alard, O., Griffin, W. L., Lorand, J. P., Jackson, S. E. and O'Reilly, S. Y. (2000) Non-chondritic distribution of the highly siderophile elements in mantle sulphides. *Nature* **407**, 891–894.
- Ankudinov, A. L. and Rehr, J. J. (1997) Relativistic calculations of spin-dependent x-ray absorption spectra. *Phys. Rev. B* **56**, 1712–1716.
- Brown, G. E., Jr. and Sturchio, N. C. (2002) An overview of synchrotron radiation applications to low temperature geochemistry and environmental science. *Rev. Min. Geochem.* **49**, 1–115.
- Cabri, L. J. (2002) The platinum-group minerals. *The Geology, Geochemistry, Mineralogy and Mineral Beneficiation of Platinum-group Elements* (Cabri, L. J., ed.), *Can. Inst. Min. Metall. Petrol. Sp. Vol.* **54**, 13–129.
- Farges, F., Browen, G. and Velde, D. (1994) Structural environment of Zr in 2 inosilicates from Cameroon—mineralogical and geochemical implications. *Am. Mineral.* **79**, 838–847.
- Fleet, M. E., Liu, M. and Crocket, J. H. (1999) Partitioning of trace amounts of highly siderophile elements in the Fe-Ni-S system and their fractionation in nature. *Geochim. Cosmochim. Acta* **63**, 2611–2622.
- Hattori, K. and Cabri, L. J. (1991) Origin of platinum-group-mineral nuggets inferred from an osmium-isotope study. *Can. Mineral.* **30**, 289–301.
- Hattori, K., Cabri, L. J. and Hart, S. R. (1991) Osmium isotope ratios of PGM grains associated with the Freetown Layered Complex, Sierra Leone, and their origin. *Contrib. Mineral. Petrol.* **109**, 10–18.
- Hawthorne, F. C. (1988) Mössbauer Spectroscopy. *Rev. Mineral.* **18**, 255–340.
- Herr, W., Hoffmeister, W., Hirt, B., Geiss, J. and Houtermans, F. G. (1961) Versuch zur Datierung von Eisenmeteoriten nach der Rhenium-Osmium-Methode. *Z. Naturforsch.* **16a**, 1053–1058.
- Horan, M. F., Morgan, J. W., Walker, R. J. and Grossman, J. N. (1992) Rhenium-osmium isotope constraints of the age of iron meteorites. *Science* **255**, 1118–1121.
- Morgan, J. W. (1971) Osmium. *Handbook of Elemental Abundances in Meteorites* (Mason, B., ed.), 451–462, Gordon and Breach, New York.
- O'Day, P. A., Rehr, J. J., Zabinsky, S. I. and Brown, G. E. (1994) Extended X-ray absorption fine structure (EXAFS) analysis of disorder and multiple scattering in complex crystalline solids. *J. Am. Chem. Soc.* **116**, 2938–2949.
- Rakovan, J., Newville, M. and Sutton, S. (2001) Evidence of heterovalent europium in zoned Llallagua apatite using wavelength dispersive XANES. *Am. Mineral.* **86**, 697–700.
- Ravel, B. (2001) ATOMS: crystallography for the X-ray absorption spectroscopy. *J. Synchrotron Radiat.* **8**, 314–316.
- Shirey, S. B. and Walker, R. J. (1998) The Re-Os isotope system in cosmochemistry and high-temperature geochemistry. *Ann. Rev. Earth Planet. Sci.* **26**, 435–500.
- Smoliar, M. I., Walker, R. J. and Morgan, J. W. (1996) Re-Os ages of group IIA, and IIIA, IVA iron meteorites. *Science* **271**, 1099–1102.
- Stern, E. A. (1993) Number of relevant independent points in X-ray absorption fine-structure spectra. *Phys. Rev. B* **48**, 9825–9827.
- Stingl, T., Mueller, B. and Lutz, H. D. (1992) Crystal structure refinement of osmium(II) disulfide. *Zeitschrift fuer Kristallographie* **202**, 161–162.
- Swanson, H. E. and Tatge, E. (1953) Standard X-ray diffraction powder patterns I. National Bureau of Standards (U.S.). *Circular*, **359**, 1–95.
- Swanson, H. E. and Ugrinic, G. M. (1955) Standard X-ray diffraction powder patterns. National Bureau of Standards (U.S.). *Circular*, **539**, 1–75.
- Takahashi, Y., Shimizu, H., Usui, A., Kagi, H. and Nomura, M. (2000) Direct observation of tetravalent cerium in ferromanganese nodules and crusts by X-ray-absorption near-edge structure (XANES). *Geochim. Cosmochim. Acta* **64**, 2929–2935.
- Weiser, T. W. (2002) Platinum-group minerals (PGM) in placer deposits. *The Geology, Geochemistry, Mineralogy and Mineral Beneficiation of Platinum-Group Elements* (Cabri, L. J., ed.), *Canadian Institute of Min. Metall. and Petrol. Sp. Vol.* **54**, 721–756.
- Wilson, G. C., Rucklidge, J. C., Kilian, L. R., Ding, G.-J. and Cresswell, R. G. (1997) Precious metal abundances in selected iron meteorites: in-situ AMS measurements of the six platinum-group elements plus gold. *Nucl. Instr. Methods Phys. Res. B* **123**, 583–588.
- Zavinsky, S. I., Rehr, J. J., Ankudinov, A., Albers, R. C. and Eller, M. J. (1995) Multiple scattering calculations of X-ray absorption spectra. *Phys. Rev. B* **52**, 2995–3009.